AIP | Applied Physics Letters

Use of fluorine-doped tin oxide instead of indium tin oxide in highly efficient air-fabricated inverted polymer solar cells

Woon-Hyuk Baek, Mijung Choi, Tae-Sik Yoon, Hyun Ho Lee, and Yong-Sang Kim

Citation: Applied Physics Letters **96**, 133506 (2010); doi: 10.1063/1.3374406
View online: http://dx.doi.org/10.1063/1.3374406
View Table of Contents: http://scitation.aip.org/content/aip/journal/apl/96/13?ver=pdfcov
Published by the AIP Publishing

Use of fluorine-doped tin oxide instead of indium tin oxide in highly efficient air-fabricated inverted polymer solar cells

Woon-Hyuk Baek,[1,a)] Mijung Choi,[1] Tae-Sik Yoon,[1] Hyun Ho Lee,[2] and Yong-Sang Kim[1,b)]
[1]*Department of Nano Science and Engineering, Myongji University, Gyeonggi 449-728, South Korea*
[2]*Department of Chemical Engineering, Myongji University, Gyeonggi 449-728, South Korea*

(Received 17 January 2010; accepted 8 March 2010; published online 31 March 2010)

The stability and efficiency of organic solar cells (OSCs) were improved using thermally stable fluorine-doped tin oxide (FTO) as the bottom electrode and poly(3,4-ethylenedioxythiophene):poly(styrenesulfonate) (PEDOT:PSS) and TiO_2 as the buffer layers. The TiO_2 layer between FTO and the P3HT:PCBM active layer improved the interface characteristics for a better charge transfer. The PEDOT:PSS layer retarded the oxygen diffusion to the active layer. A maximum power conversion efficiency of 4.3% was obtained for the inverted structure of FTO/TiO_2/P3HT:PCBM/PEDOT:PSS/Ag with a stable performance, and the cell retained over 65% of its initial efficiency after 500 h. Additionally, the OSCs were fabricated using all-solution based vacuum-free processes with screen printing for the Ag electrode and the results were comparable to the device that used an evaporated Ag electrode. © *2010 American Institute of Physics*. [doi:10.1063/1.3374406]

Organic Solar cells (OSCs) with conjugated polymer and fullerene bulk heterojunction (BHJ) composites are considered promising candidates as renewable energy resources because of their light weight, low cost, and simple fabrication for large area processing. Recent advances in polymer development and processing techniques have improved the performances of OSCs up to 5% in conventional device structures using transparent conductive oxide as the anode, poly(3,4-ethylenedioxythiophene):poly(styrenesulfonate) (PEDOT:PSS) as the anodic buffer layer, poly(3-hexylthiophene) (P3HT):phenyl-C_{61}-butyric acid methylester (PCBM) as the active layer, and Al or Ag as the cathode.[1–3] However, in this structure, the interface between the acidic anodic buffer layer, PEDOT:PSS, and the common transparent electrode, such as indium tin oxide (ITO), is unstable in air, especially under humid conditions.[4] Many studies have been focused on searching alternative buffer layers, including ZnO, Cs_2CO_3, V_2O_5, and MoO_3, in the inverted BHJ solar cell structure to overcome these problems.[5–7] Anatase phase titanium oxide (TiO_2) has also been considered as a candidate for the buffer layer because of its high transparency and electron mobility. Additionally, the additional charge generation at the double heterojunction of the P3HT:PCBM and P3HT:TiO_2 interfaces makes TiO_2 a promising buffer layer for replacing PEDOT:PSS.[5]

A previous study showed that a comparable short circuit current density (J_{sc}) with conventional structure could be achieved using TiO_2 instead of PEDOT:PSS in the inverted structure.[8] However this device exhibited a poor open circuit voltage (V_{oc}) of 0.45 V and fill factor (FF) of under 44%, and device performance was improved by modifying the energy band structure of the intermaterial with PEDOT:PSS as an intermediate metal-organic material between Ag and P3HT:PCBM. Moreover, OSCs using a PEDOT-based anode as the oxygen barrier for the active layer exhibited an improved device lifetime because of the lower oxygen and water permeability.[9,10]

Although ITO is widely used in OSCs as the bottom electrode because its conductivity is better than fluorine-doped tin oxide (FTO), the high temperature annealing that is used to form the TiO_2 anatase phase degrades the conductivity of ITO.[11] In this study, a thermally stable FTO substrate was employed, along with a TiO_2 buffer layer as the electron transporting layer under the P3HT:PCBM active layer. Additionally, a PEDOT:PSS layer was used as an oxygen barrier layer on the active layer. Moreover, a screen printing method was introduced for the Ag top electrode, and the device performances were similar to an evaporated Ag electrode. Although screen printing is a commonly used industrial printing technique for large area processing, it has rarely been used in OSCs for both the active layer and the top electrode compared to the use of ink-jet printing or spray deposition.[12,13]

P3HT (Rieke Metals, inc.) and PCBM (Nano-C) (1:1 weight ratio) were separately dissolved in a chlorobenzene solvent (30 mg/ml) and stirred at 60 °C for 1 h. The TiO_2 sol-gel solution was prepared by mixing titanium (IV) ethoxide, HCl, and isopropyl alcohol. The TiO_2 solution was spin coated on to the ITO (10 Ω/square) or FTO (15 Ω/square) substrate and then sintered at 500 °C for 1 h under ambient conditions. The thickness of TiO_2 was 140 nm and was measured using surface profiler (alpha-step 500). A 140 nm thick photoactive layer (P3HT:PCBM) was deposited onto the TiO_2 layer through spin coating. PEDOT:PSS was mixed with 1% (v/v) of a Triton X-100 [$C_{14}H_{22}O(C_2H_4O)_n$] nonionic surfactant in order to deposit the hydrophilic PEDOT:PSS solution onto hydrophobic active layer. Then this solution was spin coated (40 nm) onto the hexamethylene disilazane precoated surface. Thermal preannealing was conducted at 160 °C for 5 min on a hot plate in ambient air. The Ag top electrode (100 nm) was thermally evaporated or screen printed with an active area of 0.1 cm^2. The postannealing step was conducted at 160 °C for 1 min. The final solar cell device was fabricated with a structure of ITO

a)Electronic mail: whbaek@mju.ac.kr.
b)Electronic mail: kys@mju.ac.kr.

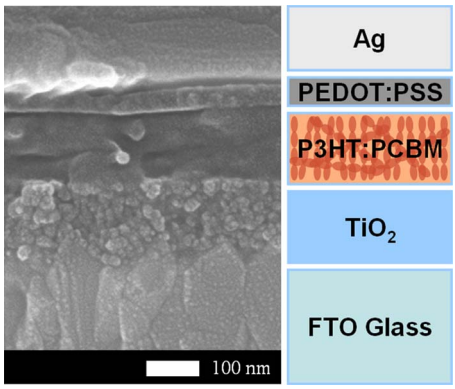

FIG. 1. (Color online) Cross section of scanning electron microscopy image of the inverted OSCs and the schematic device structure.

(FTO)/TiO_2/P3HT:PCBM/PEDOT:PSS/Ag in Fig. 1. A UV/visible spectrophotometer (Shimadzu UV-1601) was used to study the transmittance of ITO and FTO. The sheet resistance of ITO and FTO was measured using a four point probe. The current density-voltage (J-V) characteristics were measured using a J-V curve tracer (Eko MP-160) and a solar simulator (YSS-E40, Yamashita denso) under an AM 1.5 G (100 mW/cm^2) irradiation intensity. The total incident light intensity was calibrated using a pyranometer (Eko MS-802) and a standard reference silicon solar cell. The entire fabrication, storage, and measurement processes were conducted in ambient air.

Figure 2 shows the transmittance of the ITO and FTO layers on the glass before and after annealing at 500 °C for 1 h, which were the same conditions as the TiO_2 sintering. The transmittance of FTO was almost constant after annealing. On the other hand, the transmittance of ITO redshifted and was reduced to the range of 400~600 nm, which was the main absorption wavelength region of P3HT. Moreover, the sheet resistance of ITO was approximately four times (40 Ω/square) higher than the initial resistance, whereas the resistance of FTO remained almost unchanged. Therefore, FTO exhibited a better thermal stability than ITO, and these results were in agreement with previous reports.[11] These optical and electrical characteristics of FTO led to a higher incident light absorption and better charge transport properties for the devices.

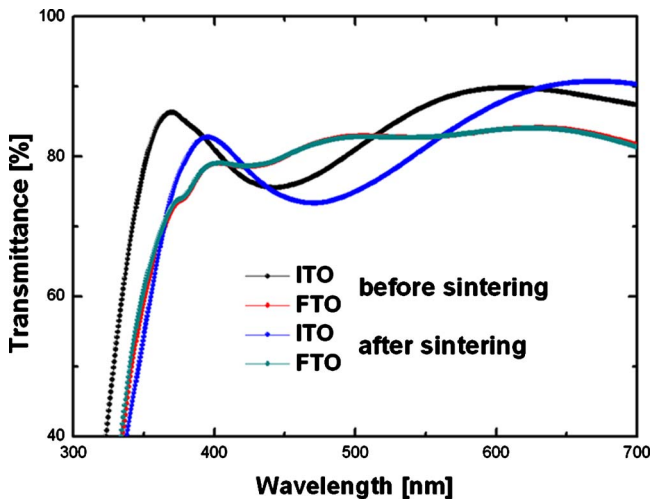

FIG. 2. (Color online) Transmittance of the ITO and FTO layers on the glass before and after annealing at 500 °C for 1 h.

TABLE I. Device performances of the inverted OSCs over a period of 500 h using ITO or FTO as the cathode and evaporated or screen printed Ag as the anode.

Cathode/anode (storage time)	PCE [%]	J_{sc} [mA/cm^2]	V_{oc} [V]	FF
ITO/evaporated Ag (0 h)	4.01	10.83	0.603	0.614
ITO/evaporated Ag (500 h)	2.02	7.65	0.580	0.455
FTO/evaporated Ag (0 h)	4.31	11.27	0.609	0.628
FTO/evaporated Ag (500 h)	2.81	8.36	0.603	0.558
FTO/screen printed Ag (0 h)	3.05	9.38	0.590	0.551
FTO/screen printed Ag (500 h)	2.15	6.92	0.570	0.545

Table I shows the photovoltaic (PV) performance of the OSCs with a structure of ITO/evaporated Ag, FTO/evaporated Ag, and FTO/screen printed Ag. The PV performance was optimized for the inverted solar cells using a 1:1 ratio of P3HT:PCBM with an ITO/evaporated Ag electrode. At these optimized conditions, the power conversion efficiency (PCE) was 4.01% and the J_{sc} was 10.83 mA/cm^2. In previous reports on the inverted structure using TiO_2 without PEDOT:PSS, the PCE was less than 1.5% with a poor open circuit voltage (V_{oc}) of 0.45 V and FF less than 44%. Although the top electrode and thicknesses of the active and buffer layers were slightly different in this study, the device performance was significantly improved by modifying the energy band structure of the intermaterial with an ambilateral conductive polymer, PEDOT:PSS, which had an intermediate work function between P3HT and Ag. Moreover, the device with FTO/evaporated Ag exhibited thermally stable optical and electrical characteristics and had a PCE of 4.31% and a J_{sc} of 11.27 mA/cm^2. Although the OSCs with FTO exhibited similar FF and V_{oc} to the OSCs with ITO, the improved efficiency and higher J_{sc} were mainly caused by the higher conductivity of FTO after sintering.

The device with FTO/screen printed Ag exhibited comparable V_{oc} and FF values to the device that contained evaporated Ag, but the J_{sc} was noticeably lower. The series resistances derived from the slope of the J-V characteristics under illumination close to the J_{sc} were 5.86 and 6.58 Ω cm^2 for the evaporated and screen printed Ag, respectively. The increased series resistance was caused by lower charge transportation for the screen printed Ag, which had worse interface properties and conductivity than the evaporated Ag. The resistivity of the screen printed Ag that was deposited on the bare glass substrate was 50~60 μΩ cm, which was ~30 times higher than the evaporated Ag (1.7~2 μΩ cm) because the Ag screen printing ink contained about 30% carbon. Although these values were lower than the resistivity of ITO (140~150 μΩ cm), the higher resistivity of the screen printed Ag reduced the charge transport. Moreover, the interfacial properties, such as the stability and the contact resistance between PEDOT:PSS and the Ag ink, were worse because of the Ag ink that was used in the screen printing. Therefore, the PV performances were lower in the screen printed devices. Nevertheless, the FTO/screen printed Ag devices exhibited a PCE of 3.05% and a J_{sc} of 9.38 mA/cm^2.

Figure 3 shows the periodically measured J-V characteristics of the OSCs with ITO/evaporated Ag, FTO/evaporated Ag and FTO/screen printed Ag. These devices were stored in

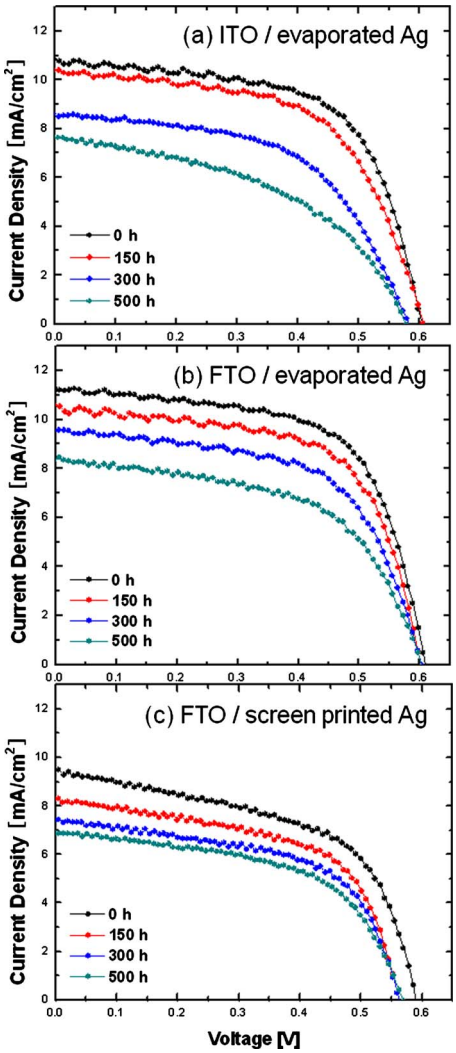

FIG. 3. (Color online) J-V characteristics of the OSCs with (a) ITO/evaporated Ag, (b) FTO/evaporated Ag, and (c) FTO/screen printed Ag at an irradiation intensity of 100 mW/cm^2 over a period of 500 h.

ambient air without encapsulation, and the device stability was periodically measured for a period of 500 h. The conventional device containing Al top electrode was unstable, and its performance was less than half of its original PCE after a day of storage. Additionally, a negligible PV performance was observed after four days.[9,14] The inverted device structure possessed a much better stability under ambient air conditions, and the FTO device retained over 65% of its original PCE after 500 h. Hau *et al.*[9] reported a better stability, and over 80% of the efficiency was retained after 40 days for a similar structure that used ZnO for the TiO_2 layer. Additionally, Lee *et al.*[14] enhanced the lifetime by two orders of magnitude over the conventional structure through the use of TiO_2 as a shielding layer in order to prevent the intrusion of oxygen and humidity into the active polymers. The device lifetime strongly depends on the storage conditions, such as the temperature and humidity. Therefore, the results in this study could not directly be compared to previous studies. Nevertheless, this work showed a considerably improved stability because of the stable interface of the inorganic FTO/TiO_2 and the PEDOT:PSS layer that was inserted under the Ag electrode as an oxygen barrier for the active layer. Although this structure still required a high temperature in order to crystallize TiO_2, the fabrication of low temperature devices on flexible substrates is possible through the further studies using the low temperature synthesis of a simple solution processed anatase TiO_2.[15]

In conclusion, the stability and efficiency of the OSCs were improved by using a thermally stable FTO electrode with an electron selective TiO_2 buffer layer and a PEDOT:PSS layer between the active layer and the top electrode in order to reduce the oxygen diffusion to the active layer. Highly efficient air-stable polymer solar cells, which retain over 65% of initial efficiency after 500 h, were obtained with a maximum PCE of 4.3% for the inverted structure of FTO/TiO_2/P3HT:PCBM/PEDOT:PSS/Ag. Moreover, the OSCs that were fabricated using vacuum-free all-solution processes with a screen printed Ag top electrode exhibited comparable PV performances to the devices using evaporated Ag.

This work was supported by Grant No. ROA-2006-000-10274-0 from the National Research Laboratory Program of the Korea Science and Engineering Foundation.

[1]K. Kim, J. Liu, M. A. G. Namboothiry, and D. L. Carroll, Appl. Phys. Lett. **90**, 163511 (2007).
[2]W. Ma, C. Yang, X. Gong, K. Lee, and A. J. Heeger, Adv. Funct. Mater. **15**, 1617 (2005).
[3]H.-L. Yip, S. K. Hau, N. S. Baek, and A. K.-Y. Jen, Appl. Phys. Lett. **92**, 193313 (2008).
[4]M. Jørgensen, K. Norrman, and F. C. Krebs, Sol. Energy Mater. Sol. Cells **92**, 686 (2008).
[5]G. K. Mor, K. Shankar, M. Paulose, O. K. Varghse, and C. A. Grimes, Appl. Phys. Lett. **91**, 152111 (2007).
[6]M. S. White, D. C. Olson, S. E. Shaheen, N. Kopidakis, and D. S. Ginley, Appl. Phys. Lett. **89**, 143517 (2006).
[7]H. Liao, L. Chen, Z. Xu, G. Li, and Y. Yang, Appl. Phys. Lett. **92**, 173303 (2008).
[8]W.-H. Baek, I. Seo, T.-S. Yoon, H. H. Lee, C. M. Yun, and Y.-S. Kim, Sol. Energy Mater. Sol. Cells **93**, 1587 (2009).
[9]S. K. Hau, H.-L. Yip, N. S. Baek, J. Zou, K. O'Malley, and A. K.-Y. Jen, Appl. Phys. Lett. **92**, 253301 (2008).
[10]M. Andersen, J. E. Carle, N. Cruys-Bagger, M. R. Lilliedal, M. A. Hammond, B. Winther-Jensn, and F. C. Krebs, Sol. Energy Mater. Sol. Cells **91**, 539 (2007).
[11]T. Kawashima, T. Ezure, K. Okada, H. Matsui, K. Goto, N. Tanabe, and J. Photoch, J. Photochem. Photobio., A. **164**, 199 (2004).
[12]C. Girotto, B. P. Rand, S. Steudel, J. Genoe, and P. Heremans, Org. Electron. **10**, 735 (2009).
[13]D. Vak, S.-S. Kim, J. Jo, S.-H. Oh, S.-I. Na, J. Kim, and D.-Y. Kim, Appl. Phys. Lett. **91**, 081102 (2007).
[14]K. Lee, J. Y. Kim, S. H. Park, S. H. Kim, S. Cho, and A. J. Heeger, Adv. Mater. **19**, 2445 (2007).
[15]N. Uekawa, J. Kajiwara, K. Kakegawa, and Y. Sasaki, J. Colloid Interface Sci. **250**, 285 (2002).